Sugar-Based Gemini Surfactant with a Vesicle-to-Micelle Transition at Acidic pH and a Reversible Vesicle Flocculation near Neutral pH

Markus Johnsson,* Anno Wagenaar, and Jan B. F. N. Engberts

Stratingh Institute, Physical Organic Chemistry Unit, University of Groningen, Nijenborgh 4, 9747 AG Groningen, The Netherlands

Received August 19, 2002 ; E-mail: M.Johnsson@chem.rug.nl

Abstract: A sugar-based (reduced glucose) gemini surfactant forms vesicles in dilute aqueous solution near neutral pH. At lower pH, there is a vesicle-to-micelle transition within a narrow pH region (pH 6.0–5.6). The vesicles are transformed into large cylindrical micelles that in turn are transformed into small globular micelles at even lower pH. In the vesicular pH region, the vesicles are positively charged at pH < 7 and exhibit a good colloidal stability. However, close to pH 7, the vesicles become unstable and rapidly flocculate and eventually sediment out from the solution. We find that the flocculation correlates with low vesicle ζ-potentials and the behavior is thus well predicted by the classical DLVO theory of colloidal stability. Surprisingly, we find that the vesicles are easily redispersed by increasing the pH to above pH 7.5. We show that this is due to a vesicle surface charge reversal resulting in negatively charged vesicles at pH > 7.1. Adsorption, or binding, of hydroxide ions to the vesicular surface is likely the cause for the charge reversal, and a hydroxide ion binding constant is calculated using a Poisson–Boltzmann model.

Introduction

By the covalent linking of two "conventional" surfactants via a spacer, a new class of surfactants, generally referred to as gemini or dimeric surfactants, has been created.[1,2] This class of surfactants provides novel and interesting opportunities to investigate surfactant aggregation properties and to test current theories on surfactant self-assembly. Furthermore, gemini surfactants can be expected to find use in various applications as, for example, in drug and/or gene delivery.[3,4]

The present study deals with the remarkable aggregation properties of a gemini surfactant **1** with carbohydrate headgroups (reduced glucose). The headgroups are connected via a short ethylene oxide spacer, and the hydrocarbon tails are oleyl chains (Figure 1). Perhaps the most important feature of **1** is the presence of two tertiary nitrogens that can be protonated, and thus, the curvature of the aggregates that are formed by this surfactant should be sensitive to the solution pH. Indeed, in previous studies from this laboratory on similar geminis but with saturated alkyl tails and $(-CH_2-)_n$ spacers, a pH-dependent vesicle-to-micelle transition has been confirmed.[4,5]

Herein, we show that the first micellar structures to form from **1** at mildly acidic pH are large cylindrical or threadlike micelles. At higher pH, we find that positively charged vesicles are formed which can be flocculated by further increasing the pH.
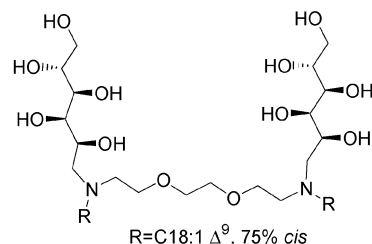

Figure 1. Structure of the gemini surfactant **1**. The cis/trans ratio was determined by ^{1}H NMR.

This flocculation/aggregation process is reversible, and the vesicles are easily redispersed by a further small increase of the hydroxide ion concentration. We show that this is due to a vesicle surface charge reversal. In line with recent results on the charging of (partially) nonionic surfactant covered surfaces in contact with aqueous solutions,[6-9] we find that the charge reversal is most likely due to the adsorption or binding of hydroxide ions to the membrane–water interface. We use a Poisson–Boltzmann model to describe the observed pH dependence of the vesicle ζ-potential and to calculate an OH$^-$ binding constant. The results display a remarkably large affinity of the gemini vesicles for hydroxide ions, and we briefly discuss the possible mechanism of OH$^-$ binding. Furthermore, recent studies on neutral glycolipid vesicles have revealed a rather

(1) Menger F. M.; Littau, C. A. *J. Am. Chem. Soc.* **1991**, *113*, 1451.
(2) Zana, R. *Adv. Colloid Interface Sci.* **2001**, *97*, 205.
(3) McGregor, C.; Perrin, C.; Monck, M.; Camilleri, P.; Kirby, A. J. *J. Am. Chem. Soc.* **2001**, *123*, 6215.
(4) Fielden, M. L.; Perrin, C.; Kremer, A.; Bergsma, M.; Stuart, M. C.; Camilleri, P.; Engberts, J. B. F. N. *Eur. J. Biochem.* **2001**, *268*, 1269.
(5) Bergsma, M.; Fielden, M. L.; Engberts, J. B. F. N. *J. Colloid Interface Sci.* **2001**, *243*, 491.

(6) Bergeron, V.; Waltermo, Å.; Claesson, P. M. *Langmuir* **1996**, *12*, 1336.
(7) Karraker, K. A.; Radke, C. J. *Adv. Colloid Interface Sci.* **2002**, *96*, 231.
(8) Stubenrauch, C.; Schlarmann, J.; Strey, R. *Phys. Chem. Chem. Phys.* **2002**, *4*, 4504.
(9) Marinova, K. G.; Alargova, R. G.; Denkov, N. D.; Velev, O. D.; Petsev, D. N.; Ivanov, I. B.; Borwankar, R. P. *Langmuir* **1996**, *12*, 2045.

similar behavior,[10,11] suggesting that our findings may be of importance for the understanding of the interactions between biologically more relevant membranes.[10-13]

Experimental Section

The synthesis of gemini **1** is outlined in the Supporting Information. All salts and reagents were of analytical grade and were used as received.

Vesicle dispersions were prepared from **1** (5 mM) at pH 6.7 by a brief tip sonication (<5 min at 35 °C) of **1** in a medium containing 5 mM each of the buffer substances Hepes, Mes, and NaAc (unless otherwise indicated). The resulting bluish (weakly turbid) dispersion was freeze−thawed (N₂(l) ↔ waterbath, 50 °C) three times, followed by extrusion through 200 nm pore-sized polycarbonate filters. Note that vesicle morphology was confirmed by cryo-transmission electron microscopy (c-TEM) (not shown).

Samples for light scattering and/or electrophoretic mobility measurements were prepared by diluting the vesicle stock solution to 0.5 mM (unless otherwise indicated) and titrating the samples to the required pH (HCl(aq) or NaOH(aq)). The pH was measured using a semi-micro ROSS combination pH electrode from Thermo Orion, U.K..

Static and dynamic light scattering (SLS and DLS) measurements were carried out at 25 °C on a Zetasizer 5000 instrument (Malvern Instruments, Ltd., U.K.) at a wavelength (λ_0) of 633 nm. The SLS and DLS measurements on micellar samples were performed at a surfactant concentration of 5 mM because of the weak scattering of these samples. The micellar samples were centrifuged for 15 min at 2000 rpm before the measurements to remove any interfering dust particles from the scattering volume. The angular dependence of the scattered light intensity was measured between $50° \leq \theta \leq 130°$, and 25 angles were measured. The setting of the scattering angle (θ) was performed via an in-built automatic angle selection system. The intensity data were corrected for background (cell and solvent) scattering and normalized using toluene as a reference standard. The autocorrelation functions obtained from DLS were analyzed using CONTIN[14] in all cases, and the measurements were performed at five different angles (50°−130°).

Electrophoretic mobility (u) measurements were carried out using the Zetasizer instrument on vesicular samples, prepared as described above, in either 15 mM buffer or 15 mM NaCl containing 0.5 mM **1**. The samples obtained after titration to the required pH were equilibrated for at least 1 h before the measurements. Results obtained after longer equilibration time (>12 h) were within experimental error identical to the results obtained after 1 h. Before each series of measurements, the Zetasizer instrument was calibrated using a ζ-potential standard solution (latex standards) supplied by Malvern Instruments, U.K.. The electric field strength in the cell was 19 V/cm, and the temperature was kept at 25 °C. The electrophoretic mobility was converted into ζ-potential using the Henry equation

$$\zeta = 3\eta u/2\epsilon_r\epsilon_0 \, f(\kappa R) \qquad (1)$$

where η, $\epsilon_r\epsilon_0$, κ, and R are the viscosity of the aqueous medium, the permittivity of water, the inverse of the Debye length, and the vesicle radius, respectively. The function $f(\kappa R)$ was set equal to 1.39 ($\kappa = 0.403$ nm^{-1}, $R = 80$ nm). The reproducibility of the mean value when measured several times on a given sample over a time period of 15 min was within ±3 mV (this was also the case when the ζ-potential was measured on separately prepared vesicle dispersions).

(10) Baba, T.; Zheng, L.-Q.; Minamikawa, H.; Hato, M. *J. Colloid Interface Sci.* **2000**, *223*, 235.
(11) Zheng, L.-Q.; Shui, L.-L.; Shen, Q.; Li, G.-Z.; Baba, T.; Minamikawa, H.; Hato, M. *Colloids Surf., A* **2002**, *207*, 215.
(12) Webb, M. S.; Tilcock, C. P. S.; Green, B. R. *Biochim. Biophys. Acta* **1988**, *938*, 323.
(13) Webb, M. S.; Green, B. R. *Biochim. Biophys. Acta* **1990**, *1030*, 231.
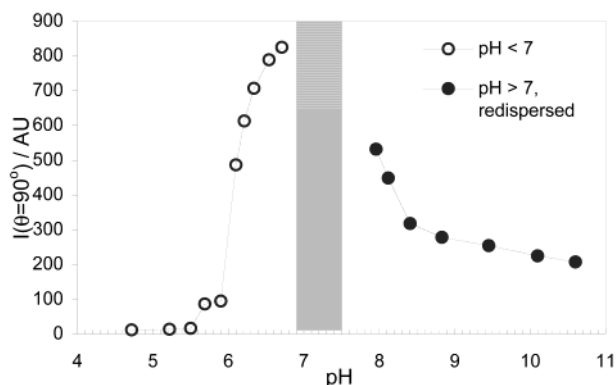(14) Provencher, S. W. *Comput. Phys. Commun.* **1982**, *27*, 229.

Figure 2. Scattered light intensity at $\theta = 90°$ as a function of pH of samples containing 0.5 mM **1** (25 °C). The hatched area indicates the pH region where a rapid vesicle flocculation takes place.
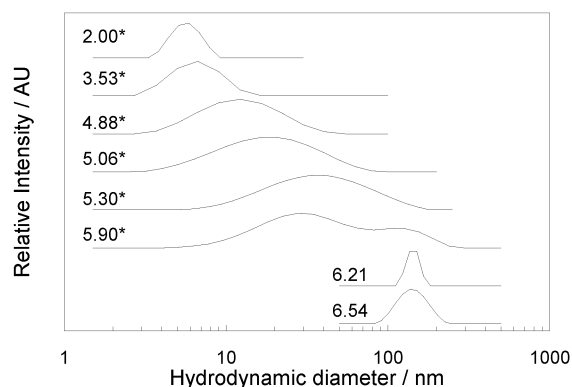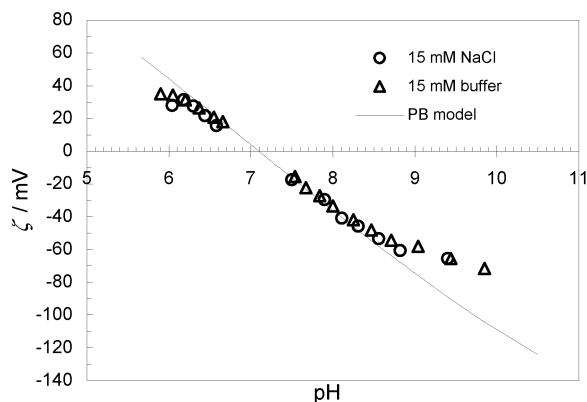

Figure 3. Size distributions obtained at $\theta = 90°$ as a function of pH (indicated in the figure) of samples containing 0.5 mM or 5 mM* of **1** (25 °C).

Results and Discussion

To obtain an overall view of the aggregation behavior of **1**, aliquots of the vesicle dispersion were titrated (HCl(aq) or NaOH(aq)) to the required pH and equilibrated overnight at 25 °C. The scattered light intensity was then measured at $\theta = 90°$. As shown in Figure 2, the intensity decreased rapidly as the pH was lowered from pH 6.7 to below pH 5. Below pH 5.6, the samples were optically clear, indicating complete micellization. Macroscopically, the samples prepared around pH 5.6 were relatively viscous and even more so when the surfactant concentration was increased to 5 mM (vide infra).

Titrating the original vesicle dispersion with NaOH resulted in a rapid vesicle flocculation around pH 7. However, the flocculated vesicles could be easily redispersed at pH values above 7.5, resulting in dispersions with the same general appearance (turbid/bluish) as the original dispersion at pH 6.7. Note that the flocculation/redispersal process was found to be completely reversible.

To make the picture more quantitative, we performed dynamic light scattering measurements as a function of pH. In Figure 3, we have plotted a selection of size distributions obtained at different pH values. Starting in the "vesicular pH region", we obtained a monomodal, relatively narrow size distribution with a mean vesicular diameter of ~160 nm. However, at pH 5.9, the size distribution became broad and bimodal. Together with the dramatic decrease of the scattered light intensity (Figure 2), the results indicate the onset of micelle formation at pH 6.0 ± 0.1. The samples became optically transparent at pH < 5.6

Figure 4. ζ-Potential as a function of pH for vesicles formed from **1** in either 15 mM buffer or 15 mM NaCl (25 °C). The fully drawn line represents the model calculations.

with broad size distributions at pH values between 5 and 5.6. The samples also became viscous relative to the original vesicle dispersion. When taken together, the results show that the vesicle-to-micelle transition occurs at pH values between 6.0 and 5.6 and that the first micellar structures possess a cylindrical shape. The mean *apparent* hydrodynamic *radius* (R_h) obtained for the micelles at pH 5.3−5.5 was 22 nm. We also observed a significant angular dependence of the scattered light intensity in this pH region consistent with large micelles. Using the Guinier approximation,[15] the angular dependence can be described by

$$I(\theta) \propto \exp(-q^2 R_g{}^2/3), \quad (qR_g << 1) \qquad (2)$$

where q is the scattering vector ($q = (4\pi n_s/\lambda_0)\sin(\theta/2)$, where n_s is the refractive index of the solution) and R_g is the radius of gyration. Fitting the obtained intensity data to the Guinier expression yielded $R_g \approx 42$ nm at pH 5.3. The ratio $R_g/R_h \approx 1.9$ provides further evidence for the formation of cylindrical micelles.[16]

Below pH 5, there was a negligible angular dependence of the scattered light intensity and the size of the micelles decreased significantly (Figure 3). Only small micelles with a mean hydrodynamic diameter of 5−6 nm were observed at pH 2.

The samples obtained after vesicle redispersal at pH > 7.5 displayed a monomodal size distribution throughout the entire pH range (pH 7.5−11). The mean size was essentially identical to that before flocculation, (∼160 nm) thus ruling out vesicle fusion as a possible outcome of the flocculation.

According to the classical DLVO theory of colloidal stability, the vesicles should become unstable with respect to aggregation/flocculation in the limit of low surface charge density where the attractive van der Waals interactions dominate.[17] Indeed, when measuring the electrophoretic mobility of the vesicles as a function of pH, the macroscopically observed flocculation coincided with low ζ-potentials, as shown in Figure 4. Figure 4 also shows why the vesicles could be redispersed at high pH, since the vesicles acquired a substantial *negative* charge by the addition of hydroxide ions. Note that this was not due to

adsorption of any of the buffer substances used, since measurements in 15 mM NaCl yielded essentially identical results (Figure 4).

It appears that the only reasonable explanation for the charge reversal is the adsorption or binding of OH⁻ to the vesicle surface. In fact, recent studies have suggested OH⁻ binding to a variety of "neutral" surfaces,[6−11] and in particular, we note the studies where the binding of hydroxide ions to neutral glycolipids resulted in negatively charged vesicles.[10,11]

To model the observed behavior, we have used a Poisson−Boltzmann model (cell model),[18] assuming that the surface potential governs the local surface concentration of ions and that there is a local equilibrium between the free ions adjacent to the vesicle surface and the bound ions on the surface. Furthermore, we assume that every surfactant molecule can bind two protons and one OH⁻ and that the headgroup area is 110 Å²[.5] With these assumptions, we solved the Poisson−Boltzmann equation in the spherical geometry ($R = 80$ nm) numerically for a given surface charge density. We then calculated the pH for which the same surface charge density was obtained with a particular set of binding constants. The details of the model can be found in the Supporting Information.

Using $K_1 = 10^{8.3}$ and $K_2 = 10^{5.8}$ for the binding of protons to the amine binding sites N(1) and N(2), respectively, and $K_{OH} = 10^{8.83}$ for the binding of OH⁻ to the sugar headgroup (or surface binding site, vide infra) (S), we obtain a satisfactory fit to the experimental data (Figure 4).

Note that the calculated potential is the surface potential which is not exactly the same as the ζ-potential.[17] Therefore, part of the discrepancy between theory and experiment is due to this difference. Nevertheless, the calculated K_{OH} corresponds to a binding Gibbs energy of ∼$20k_BT$ per bound OH⁻ (in terms of the short-ranged specific interaction), which is close to previously found Gibbs energies for OH⁻ binding to glycolipids[10] and to emulsion droplets.[9]

It is important to realize that the derived proton binding constants (K_1 and K_2) do *not* mean that N(1) and N(2) are 50% occupied (protonated) at pH 8.3 and pH 5.8, respectively, as would normally be the case for an acid, free in solution, with the same pK_a. The reason is that the proton concentration at the vesicle surface depends on the surface potential, meaning that the proton concentration is elevated at the negatively charged surface compared with that of the bulk and that the opposite is true for positively charged vesicles. This behavior is displayed more clearly in Figure 5, where we have plotted the fraction of occupied binding sites according to the model calculations. As can be seen, the S-sites (binding of OH⁻) are essentially fully occupied over the investigated pH range, which is due to the high OH⁻ binding constant (K_{OH}). Again, we emphasize that a similar behavior was found for neutral glycolipid vesicles which were determined to be negatively charged at pH values as low as pH 3.6.[10] It is also evident that the fraction of occupied N(1)-sites is increasing rapidly, whereas the fraction of occupied N(2)-sites is low throughout the studied pH range.

Interestingly, the fraction of protonated N(2) starts to increase significantly around pH 6, which is exactly the pH where we observe the onset of micelle formation. However, the fraction

(15) Guinier, A.; Fournet, G. *Small Angle Scattering of X-rays*; Wiley: New York, 1955.

(16) Schurtenberger, P.; Cavaco, C. *Langmuir* **1994**, *10*, 100.

(17) Evans, D. F.; Wennerström, H. *The Colloidal Domain: Where Physics, Chemistry, Biology and Technology Meet*; VCH Publishers Inc.: New York, 1994.

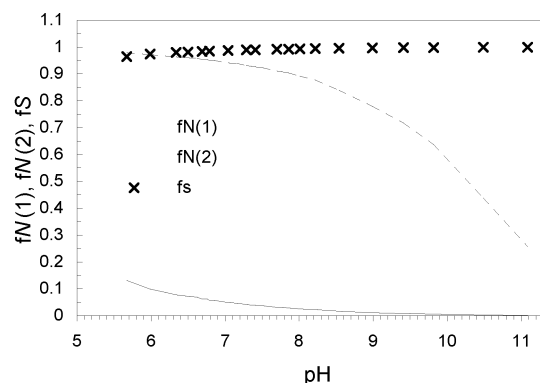(18) Gunnarsson, G.; Jönsson, B.; Wennerström, H. *J. Phys. Chem.* **1980**, *84*, 3114.

Figure 5. Fractions of protonated N(1) (fN(1), - - - -), of protonated N(2) (fN(2), —), and of occupied OH^- binding sites S (fS, ×) as a function of pH. The data are based on the model calculations.
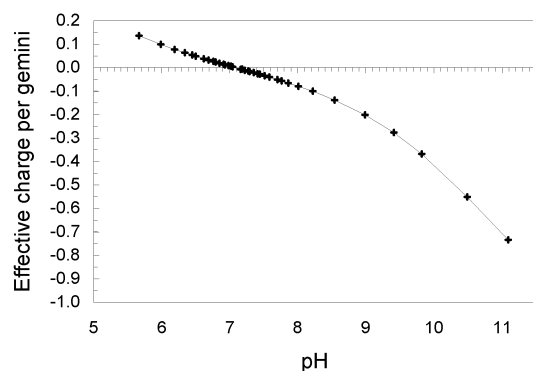

Figure 6. Effective charge per gemini surfactant as a function of pH. The data are based on the model calculations.

of protonated N(2) at pH 6 is only about 10% (thus only about 10% of the gemini **1** molecules at the vesicle surface are *doubly* protonated, since the fraction of protonated N(1) is almost 100% at pH 6). Apparently, this modest degree of protonation is enough for changing the preferred aggregate structure from vesicles to cylindrical micelles. We also note the fact that as the pH is lowered further (pH < 6), there should be a significant change in the protonation degree of N(2) which in turn should result in a moderation of aggregate size and curvature. Indeed, this is confirmed by the DLS results presented in Figure 2, which show that the size of the micelles is decreasing significantly with decreasing pH.

It may also be noted that the data in Figure 5 show why the vesicles become negatively charged above pH 7.1, since the fraction of bound OH^- is larger than the fraction of protonated N(1) and N(2) above this pH. This is more clearly displayed in Figure 6, where we have plotted the effective charge per surfactant molecule in the studied pH interval. We emphasize that this result is based on our assumption of equal binding site areas ($a_{surf} = 110 \text{ Å}^2$) for both protons and hydroxide ions.

A final feature to note is that although the (absolute) effective charge per surfactant is higher at high pH (pH > 8) than at pH 6, the DLS results reveal that only vesicles are present in the high pH range (pH 7.5–11, not shown). Thus, it is evident that electrostatics alone cannot explain the protonation-driven micelle formation at pH 6. It is likely that, besides the increased

electrostatic repulsion, protonation of N(2) results in more subtle changes of the interactions between the gemini headgroups at the membrane–water interface. For example, a conformational change of the gemini headgroup upon protonation of N(2) could be of importance.

Finally, we briefly discuss the possible mechanism of the OH^- binding. Our original hypothesis was that specific interactions between the gemini sugar headgroup and OH^- are responsible for the charge reversal of the vesicles. The satisfactory agreement between the experimental data and the model calculations suggests a 1:1 binding, thus pointing toward the sugar part as responsible for the binding. However, the available data in the literature reveal that OH^- binding to *nonionic* surfactant-covered surfaces in water seems to depend little on the identity of the nonionic surfactant headgroup.[6–9] In fact, it is a general observation that increasing the surfactant surface excess actually decreases the surface charge density, thus indicating a competition between surfactant and OH^- for surface adsorption sites.[6–9] These observations clearly speak against a sugar-induced binding of OH^- and instead favor a mechanism based on the special properties of hydrophobic surfaces in contact with water. Marinova et al.[9] suggested that the specific binding of OH^- to oil droplets in water may be due to restricted water motion in the interfacial region, thus allowing a more pronounced hydrogen bonding between the interfacial water molecules and the OH^- ions. Unfortunately, any interpretation based on a (hydrophobic)surface-induced water structure that may provide favorable interactions with OH^- is difficult to prove or disprove because of the extreme difficulties in experimentally verifying the existence of such a water structure. However, the possibility that the binding of hydroxide ions to vesicles of gemini **1** is due rather to the special properties of the membrane-(hydrocarbon)–water interface than to a specific interaction between the sugar headgroup and OH^- should clearly be considered in future studies. Studies on structurally related gemini surfactants are currently being undertaken to elucidate which factors or structural features are important for the OH^- binding.

In conclusion, we have shown that the gemini surfactant **1** displays unprecedented aggregation behavior with a vesicle-to-micelle transition within a very narrow "pH window". Furthermore, the specific binding of OH^- to the vesicular surface, leading to vesicle surface charge reversal and redispersal of flocculated vesicles, was shown and quantified using a Poisson–Boltzmann model. The use of this and similar gemini surfactants[4] in drug and gene delivery is currently under further investigation.

Supporting Information Available: Synthesis of the gemini surfactant and details of the Poisson–Boltzmann model. This material is available free of charge via the Internet at http://pubs.acs.org.

JA028195T